QUESTA E' LA VERSIONE REFERATA DI QUELLA PUBBLICATA IL 14/11/2017; https://www.sciencedirect.com/science/article/pii/S0022231317312061

Synthesis and study of three hydroxypyrazole-based ligands: a ratiometric fluorescent sensor for Zn(II)

Mauro Formica,[a] Gianfranco Favi,[b] Vieri Fusi,*[a] Luca Giorgi,*[a] Fabio Mantellini,[b] Mauro Micheloni.[a]

[a]*Department of Pure and Applied Sciences, University of Urbino, P.zza Rinascimento 6, I-61029 Urbino, Italy. Tel/Fax: +39-0722-304884.Email: luca.giorgi@uniurb.it*

[b]*Department of Biomolecular Sciences, University of Urbino, Via i Maggetti 24, I-61029 Urbino, Italy.*

Keywords: Zinc sensor, fluorescence, ratiometric sensor, 5-hydroxy-1*H*-pyrazol, ESIPT

Abstract

The coordination and photochemical properties of three hydroxypyrazole-based ligands - *tert*-butyl 2-[1-[3-(4-cianophenyl)-5-hydroxy-1-phenyl-1H-pyrazol-4-yl]ethylidene]hydrazinecarboxylate (**L1**), *tert*-butyl 2-[1-[3-(3,5-bis(trifluoromethyl)phenyl)-5-hydroxy-1-phenyl-1H-pyrazol-4-yl]ethylidene]hydrazinecarboxylate (**L2**), and *tert*-Butyl 2-[1-[3-(phenantrene-9-yl)-5-hydroxy-1-phenyl-1H-pyrazol-4-yl]ethylidene]hydrazinecarboxylate (**L3**) - are

reported. The ligands are fluorescent and able to coordinate a Zn(II) ion in a water/acetonitrile solvent with concomitant cheto-enol tautomerism, giving rise to large Stokes shifts in the emission spectra. Ligand **L1** has a peculiar double emission and can be exploited as a ratiometric fluorescent sensor.

Introduction

Zinc is the most ubiquitous of the trace elements involved in the metabolism of human beings, and its physiological importance has long been recognized.[1-5] Zinc is needed by more than 100 specific enzymes for their catalytic functioning,[6] and it also plays a part in many biochemical pathways and has multiple roles in the perpetuation of genetic material.[7] Zinc also affects both non-specific and specific immune factors, such as the integrity of the epithelial barrier and the function of neutrophils, monocytes, macrophages and lymphocytes.[8,9,10] Due to its primary biological importance, and because several diseases can be ascribed to its deficiency[11-13] or over-exposure,[14-16] many health organizations have convened expert committees to develop estimates of human zinc requirements.[17,18]

Determining the precise amount of zinc present in living systems is not easy. As a result, the development of new, non-invasive, fast systems to estimate its levels in humans is still an open field of research.[20,21]

In this context, developing fluorescent chemosensors with a high selectivity for Zn(II) in an aqueous solution is an urgent and important goal in analytical chemistry. This is because fluorescence is a fast, simple and non-invasive analytical method that is particularly suitable for *in vivo* applications. To achieve this aim, research needs to be conducted on the design and synthesis of chemosensors that are able to selectively bind

a specific substrate undergoing concomitant changes in its light absorption and/or emission properties.[22]

A typical Zn(II) sensor contains a polyamine as a binding moiety, with a linear or macrocyclic topology,[23-27] linked to a photoactive aromatic group. Most zinc sensors act through a photo-induced electron transfer (PeT) mechanism, i.e. in the metal-free form the amine moieties transfer their electron to the fluorophores in the excited state, thus quenching the fluorescence emission. When the zinc ion is coordinated to the receptor, the lone pairs of the nitrogen atoms are stabilized and this non-radiative electron transfer is suppressed. As a consequence, the emission strongly increases.[22,26,27] PeT-based sensors are perturbed by the pH, and the protonation of the polyamine receptor in fact produces false positive signals.

To circumvent this problem, other sensors based on different mechanisms of the signal transduction have been proposed,[22] for example twisted intramolecular charge transfer (TICT) sensors in which the metal ion chelation prevents the free rotation of a sigma-bond;[28] or fluorescent resonance energy transfer (FRET) in which the coordination to the metal ion changes the conformation of a ligand with two fluorophores, thus enabling energy to be transferred between them.[29] More recently, an excited state intramolecular proton transfer mechanism (ESIPT) was demonstrated. This concept is characteristic of molecules that possess an intramolecular hydrogen bond between a proton-donor group, for example a hydroxyl group, and a hydrogen-bond acceptor moiety, for instance an imine, hydrazine or hydrazide group, forming a five- or six-membered ring. Excitation of these systems can induce tautomerizaton, giving rise to a conjugate cheto form and a high Stokes shift of about 6000-12000 cm^{-1}.[30,31]

4-Acyl-5-hydroxypyrazoles and their derivatives, such as Shiff bases or hydrazones

(semicarbazone and thiosemicarbazone derivatives), are reported to behave as effective chelating and extracting reagents for many metal ions.[32] They are also the focus of research as potential antifungal agrochemicals and are widely used in medicine as antivirals, antipyretic analgesics and anti-inflammatories.[33,34] Furthermore, they are known to exhibit extensive solid-state photo-tautomerism.[35-37] These systems merge the capacity to coordinate metal ions with ESIPT features due to the cheto-enol tautomerization of the 5-hydroxypyrazole to the 5-pyrazolone moiety[38,39] (Scheme 1). They could thus be regarded as promising fluorescent sensors for Zn(II) determination. This paper describes the coordination and photochemical properties of three hydroxypyrazole-based ligands (Chart 1) in relation to Zn(II) ions, one of which has a peculiar double-band emission.

Chart 1.

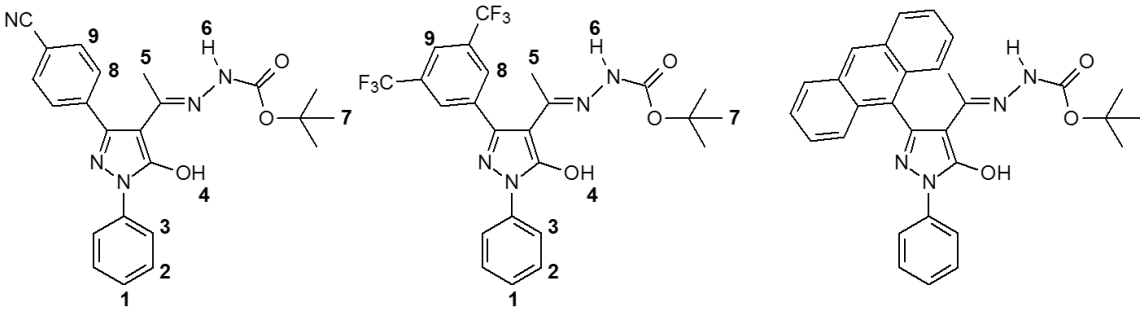

Experimental part

Synthesis and Characterization

In this study, we synthesized three differently substituted 3-aryl-hydroxypyrazole 4-hydrazones **L1-L3**, which exhibit reversible enol-keto isomerization in the solution

state. Their preparation was realized according to our previous procedure[40] from N-aryl hydrazones **1a-c** and 1,2-diaza-1,3-diene **2** through a base (NaH) promoted Michael addition/cyclization pathway (Scheme 1). Following this strategy, aromatic residues such as 4-cianophenyl, 3,5-bis(trifluoromethyl)phenyl and 9-anthracenyl were introduced at the C3 position of the pyrazole ring.

Scheme 1

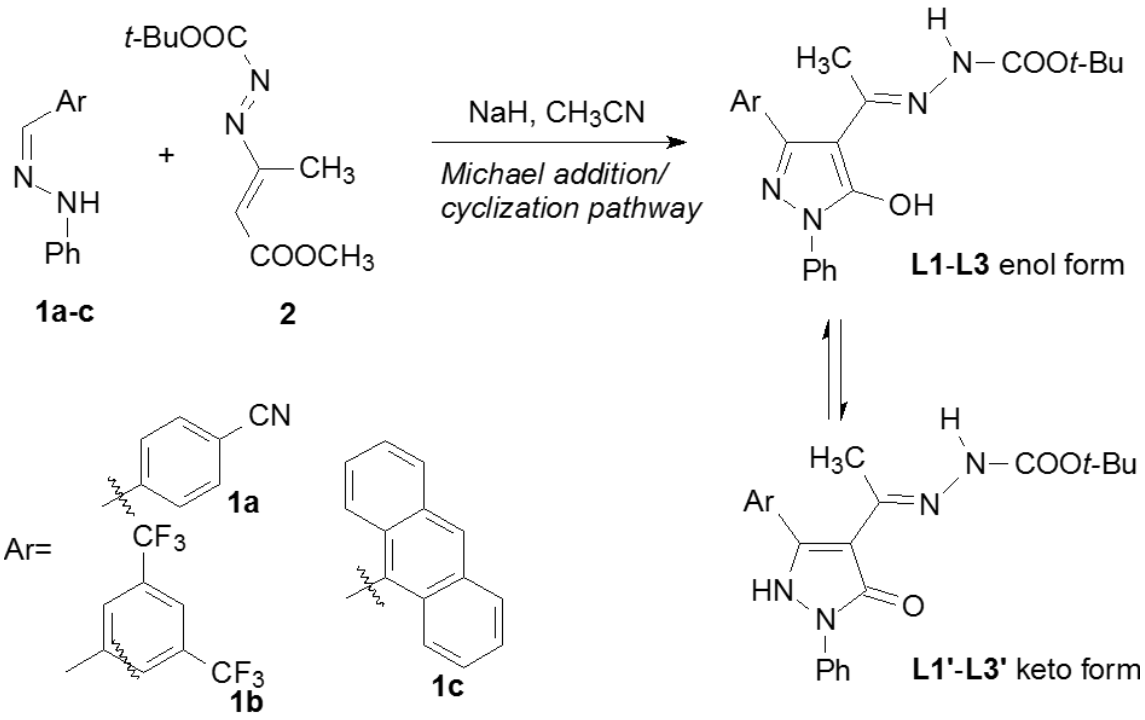

tert-Butyl 2-[1-[3-(4-cianophenyl)-5-hydroxy-1-phenyl-1H-pyrazol-4-yl]ethylidene]hydrazinecarboxylate **(L1):** Pyrazole **L1** was prepared according to known literature procedure.[40] The chemical-physical data of compound **L1** are in agreement with those reported.[40]

Yield, 65%. Pale yellow solid; mp: 126–128 °C; ^{1}H NMR (400 MHz, $CDCl_3$, 25 °C): δ = 1.47 (s, 9H), 2.00 (s, 3H), 7.07 (s, 1H), 7.20 (t, *J* = 7.2 Hz, 1H), 7.40 (t, *J* = 7.6 Hz, 2H), 7.62 (d, *J* = 8.0 Hz, 2H), 7.72 (d, *J* = 8.0 Hz, 2H), 7.98 (d, *J* = 7.6 Hz, 2H), 12.46

(bs, 1H); ^{13}C NMR (100 MHz, $CDCl_3$, 25 °C): δ = 15.4, 28.1, 83.1, 98.8, 112.7, 118.4, 119.7, 125.3, 128.8, 130.0, 132.2, 138.4, 138.9, 148.8, 154.1, 164.6, 166.9; IR (nujol): ν_{max} = 3196, 1741 cm^{-1}; MS *m/z* (%): 317 (100), 286 (83), 272 (19), 149 (55), 111 (74); anal. calcd. for $C_{23}H_{23}N_5O_3$ (417.46): C 66.17, H 5.55, N 16.78; found: C 66.31, H 5.47, N 16.66.

tert-Butyl 2-[1-[3-(3,5-bis(trifluoromethyl)phenyl)-5-hydroxy-1-phenyl-1H-pyrazol-4-yl]ethylidene]hydrazinecarboxylate **(L2):** Pyrazole **L2** was prepared according to known literature procedure.[40]

Yield, 59%. Pale yellow solid; mp: 275**–**277 °C; ^{1}H NMR (400 MHz, $CDCl_3$, 25 °C): δ = 1.50 (s, 9H), 2.03 (s, 3H), 6.98 (s, 1H), 7.23 (t, *J* = 7.6 Hz, 1H), 7.43 (t, *J* = 7.6 Hz, 2H), 7.96 (s, 1H), 7.98−8.03 (m, 4H), 12.39 (bs, 1H); ^{13}C NMR (100 MHz, $CDCl_3$, 25 °C): δ = 15.4, 28.1, 83.1, 98.8, 119.8, 122.6, 123.1 (q, *J* = 271.2 Hz), 125.5, 128.9, 129.5, 131.9 (q, *J* = 33.4 Hz), 136.4, 138.4, 147.5, 154.0, 164.4, 166.5; IR (nujol): ν_{max} = 3171, 1752 cm^{-1}; MS (ESI) *m/z* = xxx $[M + H]^+$; anal. calcd. for $C_{24}H_{22}F_6N_4O_3$ (528.45): C 54.55, H 4.20, N 10.60; found: C 54.68, H 4.14, N 10.70.

tert-Butyl 2-[1-[3-(anthracene-9-yl)-5-hydroxy-1-phenyl-1H-pyrazol-4-yl]ethylidene]hydrazinecarboxylate **(L3):** Pyrazole **L3** was prepared according to known literature procedure.[40]

Yield, 67%. White solid; mp: 290 °C (charcoal); ^{1}H NMR (400 MHz, $CDCl_3$, 25 °C): δ = 1.33 (s, 3H), 1.42 (s, 9H), 6.91 (s, 1H), 7.19 (t, *J* = 8.0 Hz, 1H), 7.41 (t, *J* = 8.0 Hz, 2H), 7.44−7.53 (m, 4H), 7.91 (d, *J* = 8.0 Hz, 2H), 8.05 (d, *J* = 8.0 Hz, 2H), 8.12 (d, *J* = 8.0 Hz, 2H), 8.57 (s, 1H), 12.4 (bs, 1H); ^{13}C NMR (100 MHz, $CDCl_3$, 25 °C): δ = 13.1, 28.0, 82.9, 101.4, 119.7, 124.9, 125.5, 125.8, 126.7, 127.5, 128.4, 128.5, 128.8, 131.2, 131.3, 138.9, 147.9, 154.0, 164.8, 167.6; IR (nujol): ν_{max} = 3191, 1721 cm^{-1}; MS (ESI) *m/z* = xxx $[M + H]^+$; anal. calcd. for $C_{30}H_{28}N_4O_3$ (492.57): C 73.15, H 5.73, N 11.37; found: C 73.28, H 5.78, N 11.29.

Solution studies

UV absorption spectra were recorded at 298.1 K on a Varian Cary-100

spectrophotometer equipped with a temperature control unit. Fluorescence emission spectra were recorded at 298.1 K on a Varian Cary-Eclypse spectrofluorimeter and the spectra are uncorrected. ^{1}H and ^{13}C NMR spectra were recorded at 298.1 K on a Bruker Avance instrument, operating at 400.13 and 100.61 MHz, respectively.

Results and discussion

Spectrophotometric, spectrofluorimetric and NMR studies were carried out to evaluate the properties of **L1-L3** ligands with respect to metal ion coordination; and, in particular, to examine the role of the hydroxy-pyrazole fragment in the coordination of metal ions. Earlier solubility screening showed that **L1** was soluble in both hydro-alcoholic and acetonitrile/water mixed solvents, **L2** was only soluble in an acetonitrile/water mixture and **L3** was soluble in an acetonitrile/water mixture with the addition of 5% DMF. The acid-base properties of **L1** were studied in 75/25 v/v water/ethanol by way of spectrophotometric and spectrophotometric titration, while the coordination properties through the Zn(II), Cu(II), Cd(II), Ni(II) and Hg(II) metal ions of all the ligands were studied in an acetonitrile/water 90/10 solution, with the addition of a further 5% of DMF in the case of **L3**.

Ligand L1

Spectroscopic UV-vis and fluorescence studies of **L1** were carried out in 75/25 v/v water/ethanol and 90/10 v/v acetonitrile/water. The absorption spectra of the neutral ligands were quite similar in both solvent mixtures, with two main bands at about 235 and 260 nm (Figures 1 and 2). The acid-base properties of **L1** were studied in 75/25 v/v water/ethanol, which was adjusted at a pH of 1.9 with 0.1 M aqueous HCl by adding a

0.1 M aqueous NaOH solution dropwise until a pH of 12.6 was achieved. In very acid conditions, **L1** showed two absorption bands at 240 nm (ε=27700 cm^{-1} dm^3 mol^{-1}) and 287 nm (ε=19000 cm^{-1} dm^3 mol^{-1}). When the pH was increased, these bands disappeared and two new bands were revealed at 233 and 260 nm in the spectrum, reaching maximum intensity at pH=12.6, with ε=27100 and 26000 cm^{-1} dm^3 mol^{-1}, respectively, (Figure 1).

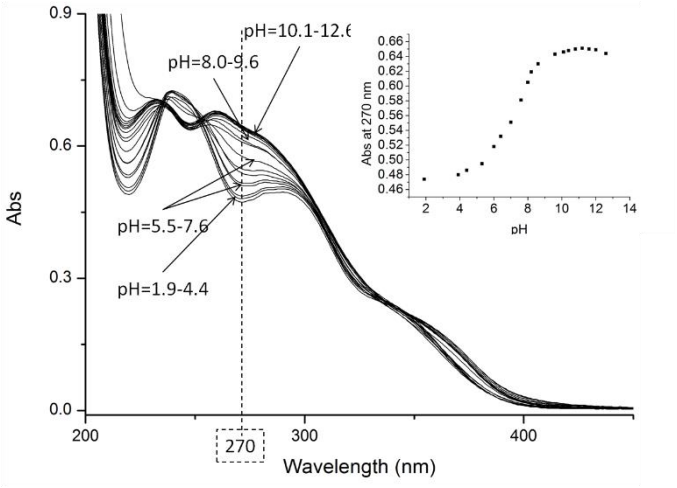

Figure 1. UV-Vis absorption spectra of **L1** registered in ethanol/water 75/25 v/v solvent mixture at various pH values. Inset: trend of the absorbance at 270 nm as a function of pH. [**L1**] = $2.7 \cdot 10^{-5}$ mol dm^{-3}.

Upon plotting the absorption trend at 270 nm versus the pH (Figure 1), it was evident that deprotonation took place starting from a pH of about 6 and ended at pH=8. Only one protonation step occurred in these experimental conditions, and given that the spectrum of the neutral **L1** dissolved in the water/ethanol change when HCl was added, but was not affected by the addition of NaOH, we concluded that **L1** was protonated in an acid environment and the protonation site probably involved the nitrogen atom N2 of

the pyrazole. The deprotonation of the OH group of hydroxypyrazole took place in a very alkaline condition, and could only be observed when solid NaOH was added (pH>12.6) to the **L1** solution. The ligand was very weakly fluorescent in this solvent, and the emission spectra were not influenced by the pH of the solution in either the presence or absence of metal ions (data not reported).

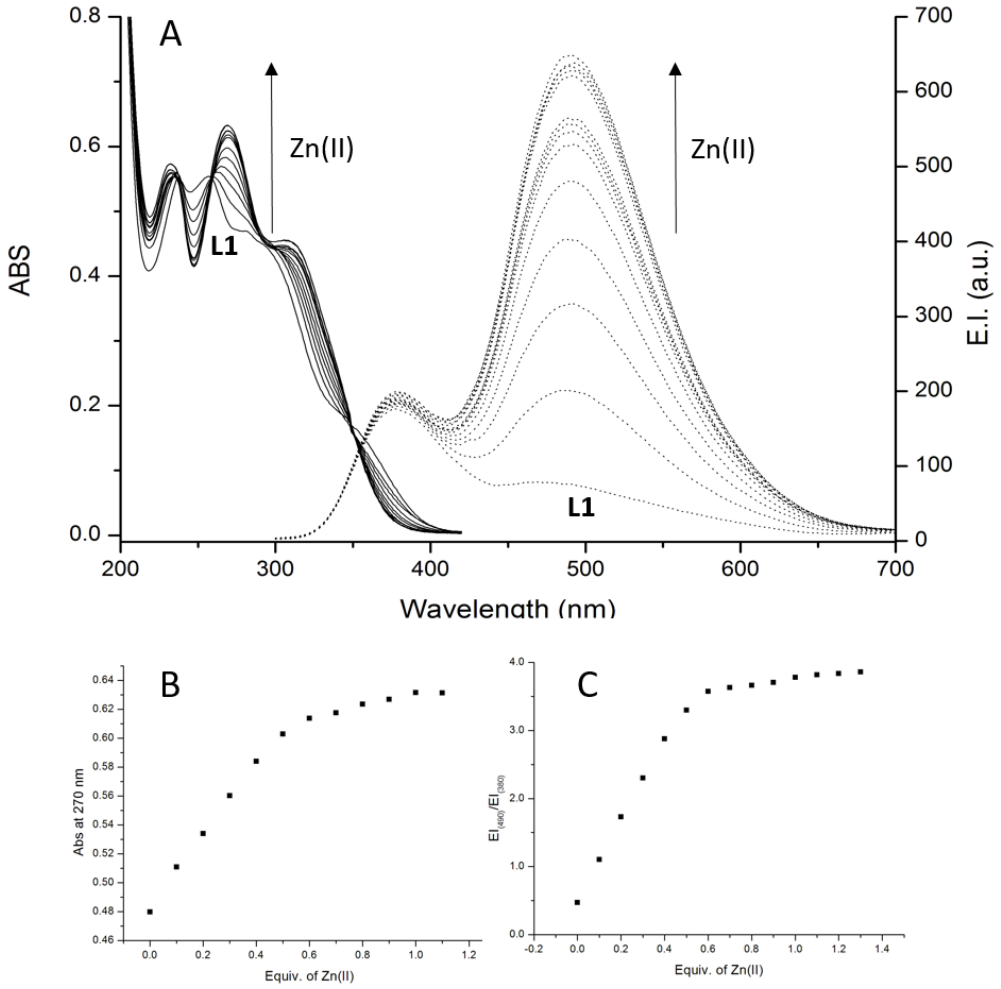

Figure 2. A. UV-Vis absorption (solid lines) and fluorescence (λ_{ex}=237 nm, dashed lines) titration of **L1** with $Zn(ClO_4)_2$ in acetonitrile/water 90/10 v/v solvent mixture. **B.** Trend of the absorbance at 270 nm as a function of equivalents of $Zn(ClO_4)_2$ added. **C.** Trend of the ratio between the emission intensity at 490 nm and those at 380 nm as a

function of equivalents of Zn(II) added. [**L1**] = $2.7 \cdot 10^{-5}$ mol dm^{-3}.

The fluorescence was probably quenched by the polarity of the solvent that promotes the charge transfer from the aromatic side arm to the excited state of the pyrazole,[41] and for this reason we studied the ligand in less polar media such as an acetonitrile/water mixture, where **L1** became fluorescent. In a 90/10 v/v solution of acetonitrile/water, the UV-vis spectrum of **L1** exhibited two absorption bands at 237 nm (ε=21000 cm dm^3 mol^{-1}) and 257 nm (ε=21000 cm^{-1} dm^3 mol^{-1}), and two shoulders at 300 nm (ε=17500 cm dm^3 mol^{-1}) and 342 nm (ε=7100 cm dm^3 mol^{-1}) (Figure 2). These absorption bands were typical of the neutral form of **L1**, as underlined by the acid-base titration described above. In these experimental conditions, the ligand was fluorescent and its fluorescence spectrum was characterized by dual emissions at 380 and 470 nm (Figure 2), which were attributed to the enol (**L1**) and keto (**L1'**) forms, respectively[42] (see Scheme 1), with the enol emission being prevalent. In order to study the interaction between **L1** and the Zn(II) ion, the UV−vis absorption and fluorescence spectra were acquired with the increasing addition of $Zn(ClO_4)_2$, and isosbestic points were observed at 237, 259, 293 and 348 nm (Figure 2). These points were consistent with a simple equilibrium system involving a free and Zn(II)-coordinated ligand. As the main change in the UV-vis absorption spectrum, the addition of Zn(II) caused the disappearance of the band at 257 nm and the emergence of a new band at 270 nm (ε=22000 cm^{-1} dm^3 mol^{-1}). Moreover, the shoulders at 300 and 342 nm disappeared, while a new shoulder appeared at 325 nm (ε=17500 cm^{-1} dm^3 mol^{-1}) and the band at 237 nm underwent a slightly blue shift up to 232 nm. The changes in the spectrum were consistent with the involvement of the hydroypyrazole ring in the Zn(II) coordination, as proposed in Scheme 2. The titration

isotherm plotting of the absorbance at 270 nm as a function of the amount of added zinc ions (0−1.2 equiv) indicated the formation of: a complex with a 1:2 Zn(II)/**L1** binding stoichiometry from a 0 to 0.5 equiv. of a metal ion; and a complex with a 1:1 stoichiometry from 0.5 to 1 equivalents (Figure 2). The fluorescence spectra of **L1**, which were acquired during the Zn(II) titration by excitation at the hysosbestic point (λ_{ex}=237 nm), revealed that the emission of the enol form at 380 nm was not perturbed when the Zn(II) ion was added, while the emission intensity of the keto form at 470 nm instead increasing by about 10 times upon the addition of 0.5 equiv. of Zn(II) red-shifting towards 490 nm. The further addition of Zn(II) did not change the emission spectrum, highlighting that a 1:2 complex was initially formed and that the transition from the 1:2 to 1:1 complex does not affect the emission (Figure 2). This supposes that both complexes $[Zn\mathbf{L1}_2]^{2+}$ and $[Zn\mathbf{L1}]^{2+}$ show the similar involvement of the hydroxypyrazole ring in the coordination of the metal ion.

The ^{1}H-NMR spectrum of **L1** recorded at 298 K in the acetonitrile-*d3* exhibited a singlet at δ=1.49 ppm, integrating nine protons that were attributed to the resonances of the H7 protons (H7, 9H), a singlet at δ=2.02 ppm (H5, 3H), a triple triplet at 7.23 ppm (H1, 1H, J_1=7.5Hz J_2=1.0Hz), a double doublet at 7.46 ppm (H2, 2H, J_1=8.6Hz, J_2=7.5Hz), a doublet at 7.72 ppm (H8, 2H, *J*=8.5 Hz), a doublet at 7.86 ppm (H9, 2H *J*=8.5 Hz) and a double doublet at 8.06 ppm (H3, 2H, J_1=8.6Hz, J_2=1.0Hz) (Figure 3A). The addition of the Zn(II) ion as perchlorate salt gave rise to the appearance of a new species with a $[Zn\mathbf{L1}_2]^{2+}$ stoichiometry in a slow exchange on the NMR time-scale with the free ligand; this species was completely formed when the 0.5 equiv. of Zn(II) was added. In this species, all the resonances of the aromatic protons, with the exception of H3, underwent a downfield shift with respect to the corresponding signals of the free ligand.

A new signal appeared at 9.60 ppm, integrating one proton, which was attributed to the H atom linked to the N2 position of the pyrazole ring in the keto form (**L1'**),[43] (Figure 3A). The H3 signal strongly shifted upfield from 8.06 to 7.55 ppm, while the resonances of H8 and H9 showed a slightly downfield shift from 7.72 and 7.86 ppm to 7.80 and 8.00 ppm, respectively (Figure 3B).

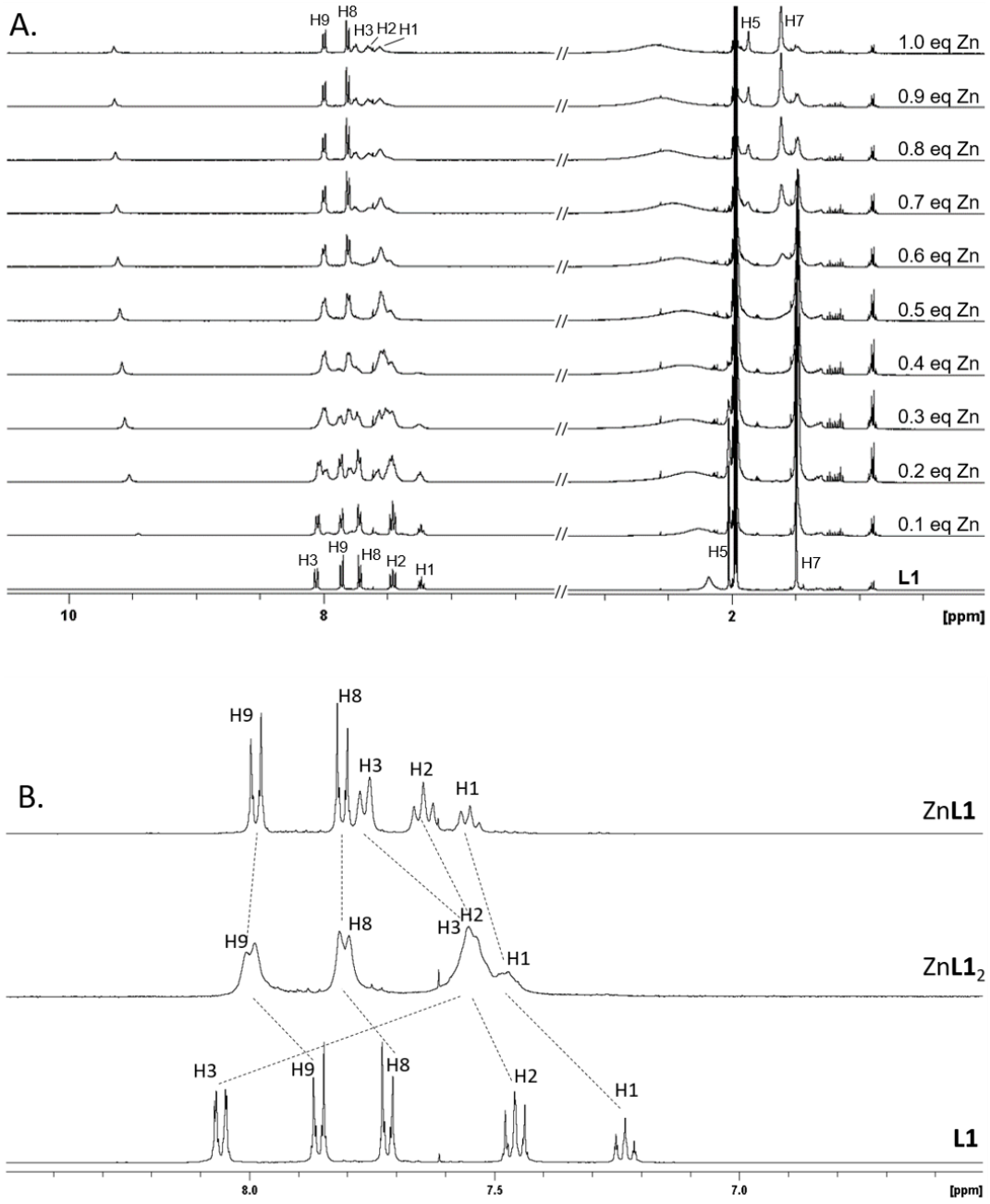

Figure 3. A. ^{1}H-NMR titration of **L1** with $Zn(ClO_4)_2$ in acetonitrile-*d3*. **B**. Aromatic signals of ^{1}H-NMR spectra of **L1**, $[Zn\mathbf{L1}_2]^{2+}$ and $[Zn\mathbf{L1}]^{2+}$ species. [**L1**]=10^{-3} mol dm^{-3}, 400 MHz, for proton labels see Chart 1.

In the aliphatic zone of the spectrum, the signal at 2.02 ppm, which was attributed to the methyl group close to the hydrazone moiety (H5), disappeared, probably because it moved under the signal of the solvent, while those at 1.49 ppm, attributed to the *tertz*-butyl fragment (H7), were not perturbed (Figure 3A). These results confirmed the involvement of the hydroxypyrazole moiety and the hydrazone group in the coordination of the metal ion in the $[Zn\mathbf{L1}_2]^{2+}$ species, as proposed in Scheme 2.

Scheme 2.

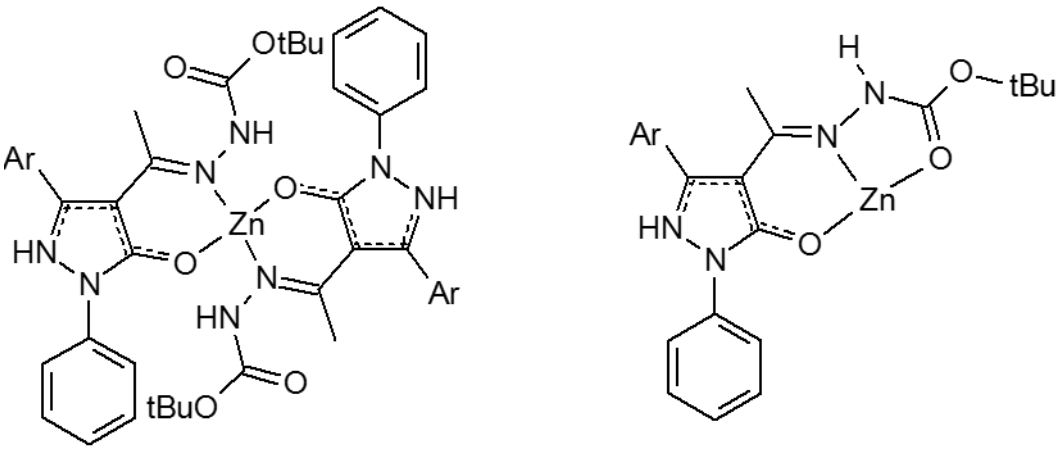

ZnL_2 **ZnL**

As the main changes involved the signals of the aromatic ring linked to the N1-atom of the pyrazole, and given the appearance of the new signal at 9.60 ppm, we concluded that the coordination of Zn(II) results in a profound change in the electronic properties of the heterocyclic N-N-O system. Analyzing both the UV-vis and NMR experiments, we

assume that Zn(II) coordination leads to a proton transfer from the OH group to the N2 atom of hydroxypyrazole that stabilizes the keto tautomer, as proposed in Scheme 2. The further addition of the Zn(II) ion led to the appearance of a mononuclear $[Zn\mathbf{L1}]^{2+}$ species whit concomitant sharpening of the ^{1}H-NMR spectrum. The signals of the H8 and H9 protons were not perturbed, while those of the three signals of the aromatic ring linked to the N atom of the pyrazole (H1, H2 and H3) became separated and well defined at 7.56, 7.65 and 7.75 ppm, respectively. An upfield shift of the H5 signal and a downfield shift of the H7 signal were also observed (Figure 3). In view of this trend, we hypothesized that the carbamate group in the 1:1 complex could contribute to the metal ion stabilization (Scheme 2), while the addition of up to one equivalent of Zn(II) does not change the spectrum further.

Taking into account the results of the UV-vis, fluorescence and NMR spectroscopic studies, the following conclusions can be drawn:

1) Zn(II) coordination mainly involves the hydroxypyrazole ring and promotes the proton transfer from the OH group to the N2 pyrazole atom.

2) Zn(II) coordination increases the emissions of the keto form, but not those of the enol form.

3) As the intensity of the enol form emission remains constant, the Zn(II) coordination does not affect the keto-enol equilibrium in the excited state.

The most plausible mechanism accounting for the peculiar zinc-induced fluorescence turn-on is that the metal coordination stabilizes the keto form in a rigid conformation in the excited state; this prevents the quenching of the fluorescence caused by the TICT effect, as schematically depicted in Figure 4.

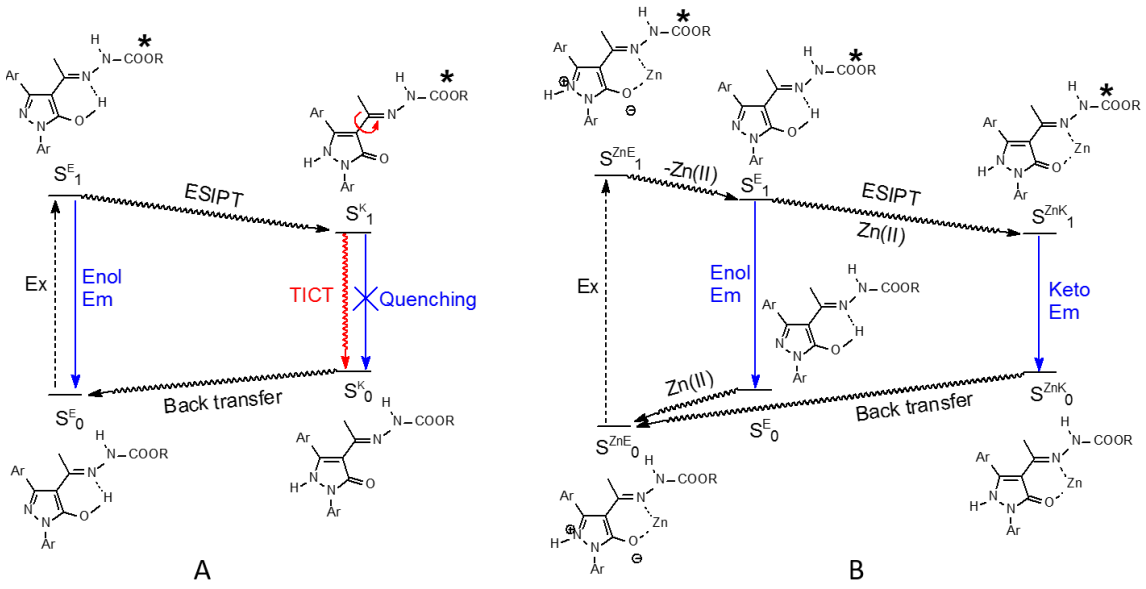

Figure 4. Proposed mechanism for the zinc-responsive fluorescence turn-on of **L1**. S^{E}_{0} and S^{K}_{0}: ground states of free enol and keto form; S^{E}_{1} and S^{K}_{1}: excited states state of free enol and keto form. S^{ZnE}_{0} and S^{ZnK}_{0}: ground states of Zn(II)-coordinated enol and keto form; S^{ZnE}_{1} and S^{ZnK}_{1}: excited states state of Zn(II)-coordinated enol and keto form of **L1**; ESIPT: excited state intramolecular proton transfer; TICT: twisted intramolecular charge transfer.

In other words, in the excited state, the free ligand **L1** achieves a slow keto-enol equilibrium due to the ESIPT process, in which the enol form is fluorescent while the keto form is quenched by a TICT effect. In the Zn(II) complex, the ligand was present in the amphiionic form and upon excitation probably lost the Zn(II) ion, giving rise to the excited **L1*** state which, via the ESIPT process, converts the excited **L1'*** state in the keto form. This could chelate the Zn(II) ion, resulting in the shift of the band from 470 to 490 nm and the suppression of the TICT effect, thus increasing the emissions of the keto-tautomer. It was possible to exploit the behaviour of **L1** with respect to the Zn(II) complexation to project a ratiometric sensor. However, when the amount of

Zn(II) was less than half of that of **L1**, the concentration of the metal ion was in fact directly proportional to the ratio between the emission intensity at 490 nm and that at 380 nm (Figure 2). The peculiarity of this ligand was that the enol emission was indifferent to the presence of Zn(II) and behaved as an *internal emission standard*, while the emission intensity of the keto form increased upon the Zn(II) coordination and acts as a chemical probe for the presence of the Zn(II) ion. As a result, the comparison between the intensity emissions of the keto form at 490 nm and those of the enol form at 380 nm (I_{490}/I_{380}) was able to provide a direct measure of the Zn(II) concentration.

The UV-vis and fluorescence titrations with other metal ions such as Cu(II), Ni(II), Cd(II) and Hg(II) were performed. All the metal ions interacted with the ligand, as highlighted by the perturbation of the absorption spectra. The addition of Cu(II), Ni(II) and Hg(II) did not change the emission spectra, while Cd(II) enhanced the emission at 490 nm (keto form), like Zn(II), but to a lesser extent (four times vs 10) (Figure 5). Competition experiments were performed by acquiring the emission spectra of **L1** in the presence of Zn(II) (1 equiv.) and another metal ion (1 equiv.) (Figure 5). The presence of Ni(II) at the same concentration as Zn(II) reduced its response by about 5% and the presence of Hg(II) by about 10%. In the presence of the Cu(II) ion, the ligand did not respond to Zn(II). This is probably because the Cu(II) complexes were more stable than the Zn(II) complex and were not emitting in the keto-tautomer. Meanwhile, the presence of Cd(II) did not affect the response of **L1** to the Zn(II) metal ion.

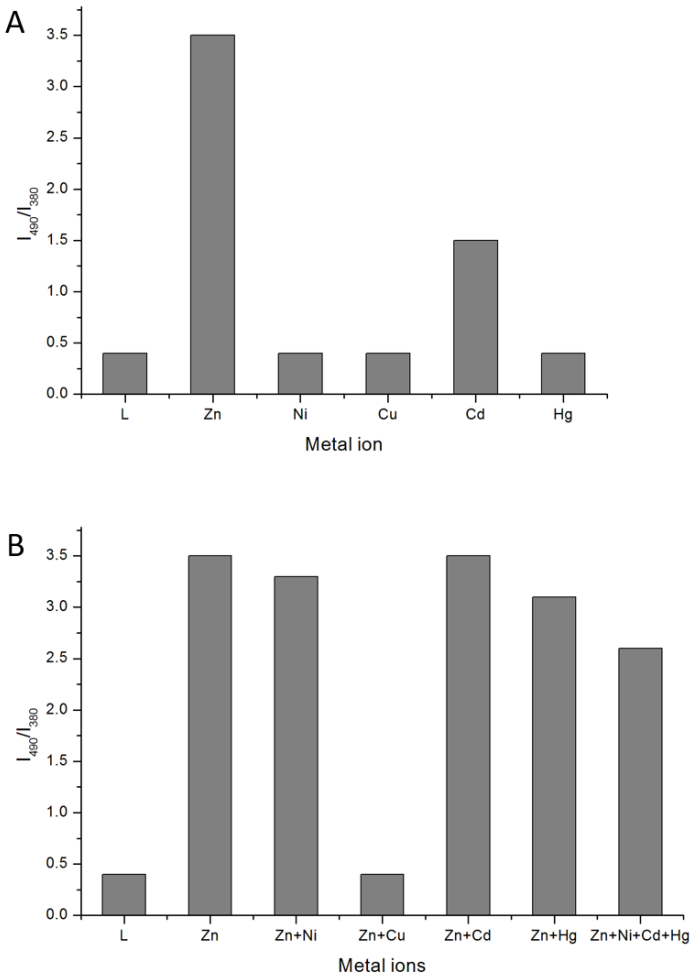

Figure 5. Ratio between the fluorescence emission intensities at 490 nm (keto band) and at 380 nm (enol band) (I_{490}/I_{380}) of **L1** (λ_{ex}=237 nm) in absence and in presence of 1 equiv. of Zn(II), Ni(II), Cu(II), Cd(II) and Hg(II) metal ion, (**A**), and in co-presence of 1 equiv. of Zn(II) and 1 equiv. of Ni(II), Cu(II), Cd(II), Hg(II) metal ions, (**B**).

Ligand L2

In the acetonitrile/water 90/10 v/v solution, **L2** had three absorption bands at 255 nm (ε=19600 cm dm^3 mol^{-1}), 281 nm (ε=18600 cm^{-1} dm^3 mol^{-1}) and 340 nm (ε=7700 cm^{-1} dm^3 mol^{-1}). The UV−vis absorption spectra were acquired with the continuous addition

of zinc ions ($Zn(ClO_4)_2$), while isosbestic points were observed at 251, 284, 302 and 347 nm (Figure 6). As the main change in the UV-vis spectrum, the addition of Zn(II) caused the disappearance of the bands at 255, 281 and 340 nm, while a new band emerged at 265 nm (ε=24500 cm^{-1} dm^3 mol^{-1}) and a shoulder at 320 (ε=13900 cm^{-1} dm^3 mol^{-1}) (Figure 6).

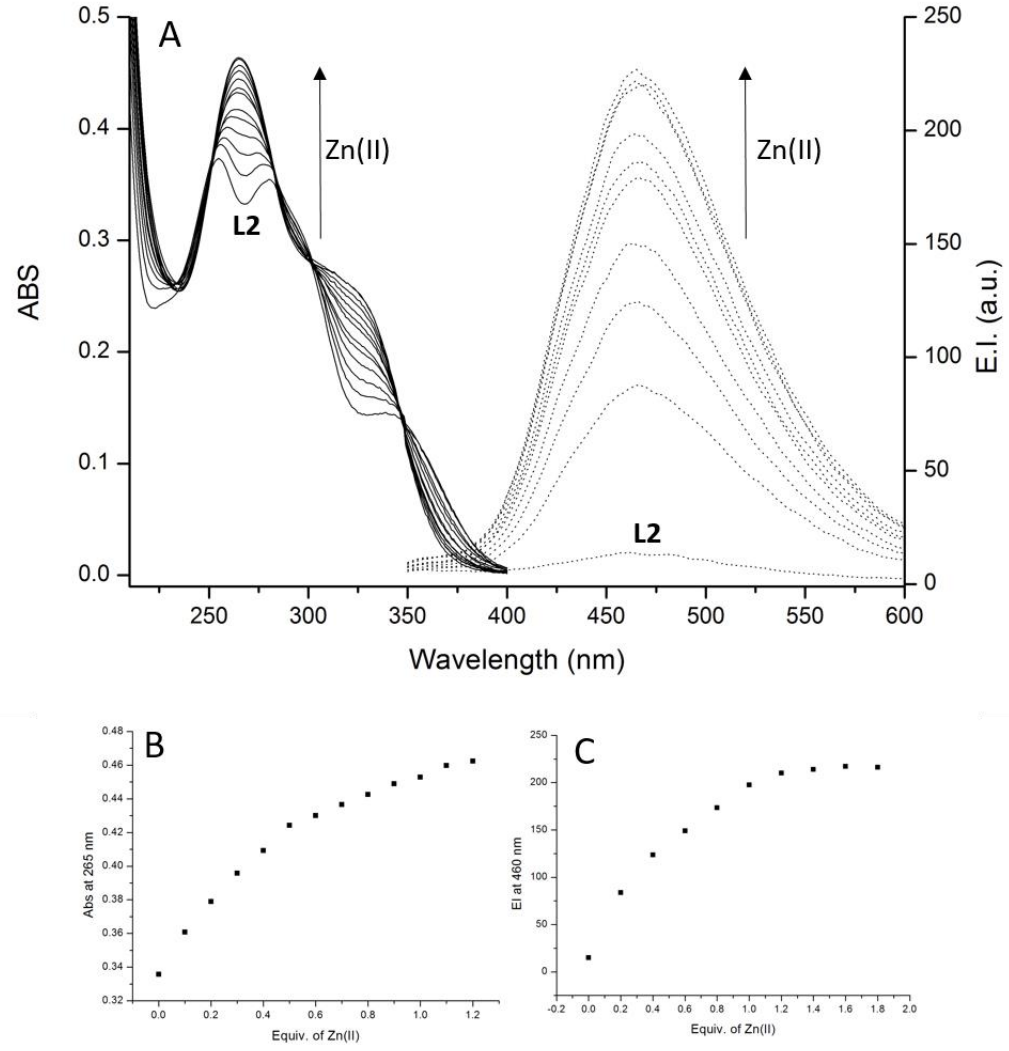

Figure 6. A. UV-Vis absorption (solid lines) and fluorescence (λ_{ex}=284 nm, dashed lines) titration of **L2** with $Zn(ClO_4)_2$ in acetonitrile/water 90/10 v/v solvent mixture. **B.** Trend of the absorbance at 265 nm and **C.** Trend of the emission intensity at 460 nm as

a function of equivalents of $Zn(ClO_4)_2$ added. [**L1**] = $2.7 \cdot 10^{-5}$ mol dm^{-3}.

The titration isotherm plotting absorbance at 265 nm as a function of the amount of added zinc ions (0−1.2 equiv) indicated the formation of: a complex with a 1:2 Zn(II)/**L1** stoichiometry up to a 0.5 equiv. of the metal ion; and a complex with a 1:1 stoichiometry from 0.5 to 1 equivalents (Figure 6). The ^{1}H-NMR spectrum of **L2** recorded at 298 K in the acetonitrile-*d3* exhibited a singlet at δ=1.49 ppm, integrating nine protons attributed to the resonances of the H7 protons (H7, 9H), a singlet at δ=2.02 ppm (H5, 3H), a triplet at 7.25 ppm (H1, 1H, *J*=7.6 Hz), a double doublet at 7.47 ppm (H2, 2H, J_1=7.6 Hz, J_2=8.6 Hz), a doublet at 8.07 ppm (H3, 2H, *J*=8.6 Hz), a singlet at 8.14 ppm (H9, 1H) and a singlet at 8.16 ppm (H8, 2H) (Figure 7). The addition of the Zn(II) ion as perchlorate salt led to the appearance of a new species in a slow exchange on the NMR time-scale with the free ligand; this was completely formed by adding a 0.5 equiv. of Zn(II). The further addition of Zn(II) formed a complex with a $[Zn\mathbf{L2}_2]^{2+}$ stoichiometry. In this species, all the resonances of the aromatic protons, with the exception of H3, underwent a downfield shift with respect to the corresponding signals of the free ligand, while a new signal appeared at 9.58 ppm, integrating one proton (Figure 7). In particular, the NMR signals of the protons H1, H2, H8 and H9 moved to 7.48, 7.53, 8.26 and 8.33 ppm, respectively, while H3 shifted upfield from 8.07 to 7.59 ppm. In the aliphatic part, the signal at 2.02 ppm, which was attributed to the methyl group close to the hydrazone group (H5), disappeared, probably because it moved under the solvent signal, but those at 1.49 ppm (H7) were not perturbed. These changes suggest the involvement of the hydroxy-pyrazole moiety and the hydrazone group in the coordination of the metal ion in the $[Zn\mathbf{L2}_2]^{2+}$ species. The further addition of the Zn(II)

ion led to the appearance of another species in which the main changes were a marked downfield shift of the aromatic H3 and aliphatic H7 signals and a upfield shift of the H5 proton. Adding up to a 1 equivalent of Zn(II) did not change the spectrum further, meaning that a 1:1 Zn(II)/ **L2** complex was formed.

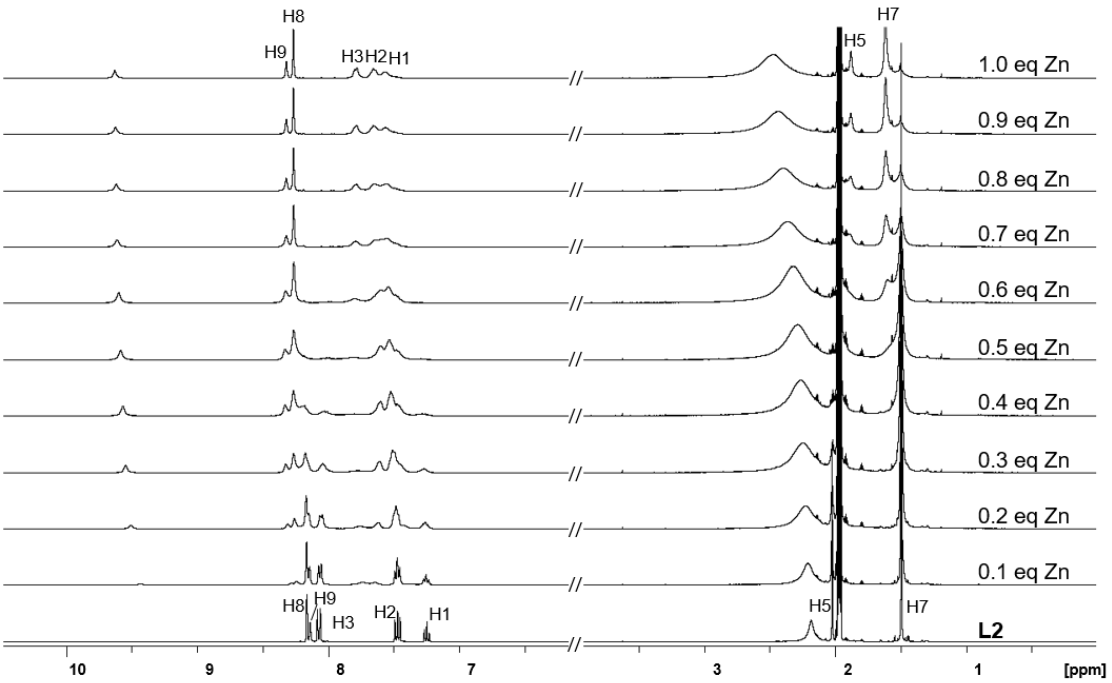

Figure 7. 1H-NMR titration of **L1** with $Zn(ClO_4)_2$ in acetonitrile-*d3*. [**L1**]=10^{-3} mol dm^{-3}, 400 mHz, for proton labels see Chart 1.

At the NMR level, the behaviour of **L2** in relation to the Zn(II) ion was quite similar to that of **L1**, and we can thus suppose an analogue coordination approach (Scheme 2).

L2 was very weakly fluorescent, with an emission band at 460 nm, which was mainly attributable to the keto form ion hydroxypyrazole ring. This increased slightly in the presence of the Zn(II) ion, while the addition of other metal ions such as Ni(II), Cu(II), Cd(II) and Hg(II) did not perturb the emission spectrum. No enol emission was observed for **L2** (Figure 6), meaning that the ESIPT effect in this case was much more

effective than in **L1**. Given the similar coordination pattern of **L2** in binding Zn(II), and in view of the fact that this did not affect the **L2** emission, this means that the photochemical behaviour of these systems was strongly influenced by the nature of the aromatic ring linked to the C3 position.

Ligand L3

In order to shift the emission intensity towards a high wavelength, the **L3** ligand, bearing an anthracene group linked to the C3-position of 5-hydroxypyrazol, has been synthesized. Due to its high insolubility in an acetonitrile/water 90/10 v/v solution, a further 5% of DMF was added. The UV-vis spectrum of **L3** had an absorption band at 287 nm (ε=15700 cm^{-1} dm^3 mol^{-1}), which was attributed to the hydroxyprazole moiety, and four absorption bands at 330 nm (ε=10800 cm^{-1} dm^3 mol^{-1}), 347 nm (ε=11700 cm^{-1} dm^3 mol^{-1}), 365 nm (ε=12200 cm^{-1} dm^3 mol^{-1}) and 385 nm (ε=10900 cm^{-1} dm^3 mol^{-1}) that were attributed to the anthracene chromophore. Due to the presence of DMF, which strongly absorbs below 270 nm, it was not possible to monitor the shape of the spectrum at a shorter wavelength than this value. The UV−vis absorption spectra were acquired with the continuous addition of zinc ions ($Zn(ClO_4)_2$), and isosbestic points were observed at 303 and 344 nm (Figure 8). The addition of Zn(II) caused the appearance of a new band at 320 nm and the disappearance of those at 287 nm. These changes were determined by the coordination of the Zn(II) ion to the hydroxypyrazole ring. The anthracene bands were not perturbed by the addition of Zn(II). The titration isotherm plotting absorbance at 320 nm as a function of the amount of added zinc ions (0−1.2 equiv) indicated the formation of a complex with a 1:1 stoichiometry ($[Zn\mathbf{L3}]^{2+}$). Unlike **L1** and **L2**, there was no evidence of a species with a $[Zn\mathbf{L3}_2]^{2+}$ stoichiometry. **L3** was

weakly fluorescent and had an emission band at about 550 nm, which was attributed to the keto form of the hydroxypyrazole ring. Meanwhile, the addition of Zn(II) slightly increased the fluorescence intensity, but did not affect the emission wavelength (Figure 8).

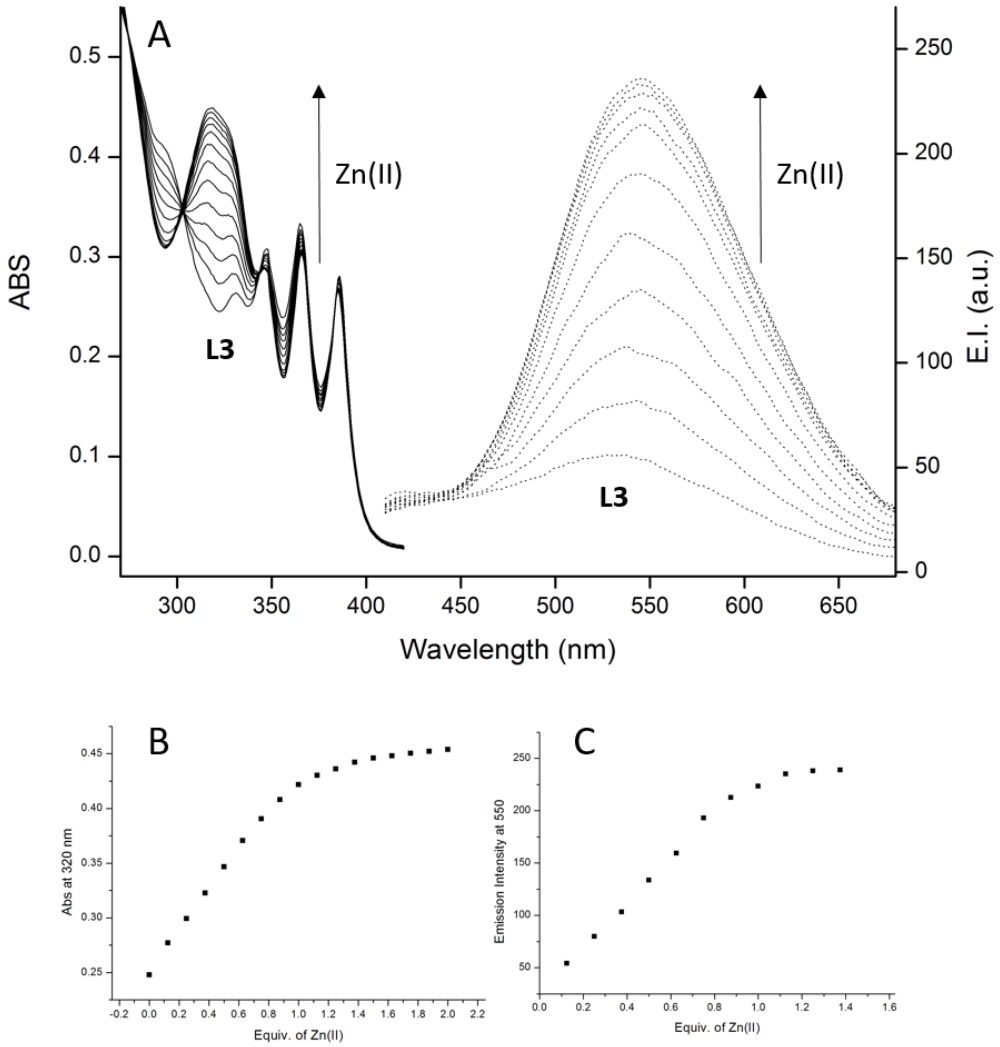

Figure 8. A. UV-Vis absorption (solid lines) and fluorescence (λ_{ex}=303 nm, dashed lines) titration of **L3** with $Zn(ClO_4)_2$ in acetonitrile/water 90/10 v/v solvent mixture withb thw addition of DMF (5%). **B.** Trend of the absorbance at 320 nm and **C.** Trend of the emission intensity at 550 nm as a function of equivalents of $Zn(ClO_4)_2$ added.

[**L3**] = $2.5 \cdot 10^{-5}$ mol dm^{-3}.

When plotting the emission at 550 nm as a function of the equivalent of the added Zn(II), we noted that a plateau was reached at a 1 equiv. of Zn(II), confirming that only a 1:1 complex was formed. Due to the conjugation with the anthracene ring, the emission band of this ligand was shifted towards the high wavelength compared to those of **L1** and **L2**, but the quantum yield was low, probably because, in this case, the TICT effect was not completely inhibited by the Zn(II) coordination.

The behaviour of **L3** with respect to Zn(II) has been confirmed by the ^{1}H-NMR titration in DMF-*d7* (data not reported), in which only a species with a 1:1 stoichiometry slow exchanging on the NMR time-scale was recorded. As **L3** in our experimental condition formed the only Zn(II)/L complex of the 1:1 stoichiometry, this could be ascribed to the presence of DMF as a co-solvent in the UV-vis and fluorescence and as a solvent in the NMR experiments. This, being more polar and with better coordinating properties than acetonitrile, could saturate the coordination sphere of the metal ion in the [Zn**L3**]$^{2+}$ species, thus preventing the formation of the 1:2 Zn(II) to **L3** complexes.[44]

Concluding remarks

We investigated the coordinative and photochemical properties of three hydrazone derivatives of 4-Acyl-5-hydroxy-1*H*-pyrazoles (which have a phenyl group at the N1-position and an aromatic moiety at C3), namely 4-cianophenyl (**L1**), 3,5-bis(trifluoromethyl)phenyl (**L2**) and 9-anthracenyl (**L3**), with respect to Zn(II) ions. **L1** and **L2** were able to bind Zn(II), giving rise to complexes with [Zn$\mathbf{L}_2$]$^{2+}$ and [Zn**L**]$^{2+}$ stoichiometry that depended on the amount of the Zn(II) ion added. Meanwhile, in the

case of **L3**, only 1:1 [Zn **L3**]$^{2+}$ species were observed. All the ligands bound the metal ion in the same coordination feature involving the oxygen atom of the hydroxypyrazole ring and the N atom of the hydrazine group. The coordination of the metal ion caused a proton transfer from the OH group to the N2 atom of the hydroxypyrazole ring, promoting the transition from the enol to the keto form, as highlighted by the UV and NMR studies. The nature of the aryl group linked at the C3 position had a great impact on the fluorescence behaviour, because it affected the emission wavelength and the extension of the TICT effect, namely the transition from the enol to the keto form at the excited state. Meanwhile, in the case of **L2** and **L3**, only the keto emission was detectable at λ_{em}=460 and 530 nm, respectively, while the emission spectra of **L1** were characterized by a double emission at 380 and 470 nm, with the former due to the enol and the latter to the keto emission. The Zn(II) coordination to **L1** caused a major increase in the fluorescence emission intensity of the keto form with the displacement of the band from 470 to 490 nm, but it did not affect either the intensity or the position of the enol band. As a result, the enol band can be regarded as an internal standard of emission. Meanwhile, the ratio between the emission intensity at 490 nm (keto) and that at 380 nm (enol) provides a direct measure of the Zn(II) level in the sample.

Acknowledgments

We would like to acknowledge the financial support provided by the Department of Pure and Applied Sciences at the University of Urbino.

References

1. A. Krezel, W. Maret, *Arch. Biochem. Biophys.*, 2016, **611**, 3−19.

2. C. J. Frederickson, J. Y. Koh, A. I. Bush, *Nat. Rev. Neurosci.*, 2005, **6**, 449−462.

3. S. C. Burdette, S. J. Lippard, *Proc. Natl. Acad. Sci.*, 2003, **100**, 3605−3610.

4. J. M. Berg, Y. Shi, *Science*, 1996, **271**, 1081−1085.

5. T. V. O'Halloran, *Science*, 1993, **261**, 715−725.

6. W. Maret, *Adv. Nutr.*, 2013, **4(1)**, 82−91.

7. A. E. Favier, *Biol. Trace Elem. Res.*, 1992, **32**, 363−82.

8. M. Maares, H. Haase, *Arch. Biochem. Biophys.*, 2016, **611**, 58−65.

9. C. Agostoni, R. Berni Canani, S. Fairweather-Tait, M. Heinonen, H. Korhonen, S. La Vieille, R. Marchelli, A. Martin, A. Naska, M. Neuhauser-Berthold, G. Nowicka, Y. Sanz, A. Siani, A. Sjödin, M. Stern, S. J. J. Strain, I. Tetens, D. Tomé, D. Turck, H. Verhagen, *EFSA Journal*, 2014, **12(5)**, 3653/1−3653/9.

10. L Rink, P. Gabriel, *Proc. Nutr. Soc.*, 2000, **59(4**), 541−552.

11. A. S. Prasad, *J. Trace Elem. Med. Biol.*, 2014, **28(4**), 357−363.

12. M. L. Ackland, A. A. Michalczyk, *Arch. Biochem. Biophys.*, 2016, **611**, 51−57.

13. K. Jurowski, B. Szewczyk, G. Nowak, W. Piekoszewski, *J. Biol. Inorg. Chem.*, 2014, **19**, 1069–1079.

14. G. J. Fosmire, *Am. J. Clin. Nutr.*, 1990, **51**, 225−227.

15. K. Konoha, Y. Sadakane, M. Kawahara, *J. Health Sci.*, 2006, **52(1)**, 1−8.

16. H. Hu, M. Bandell, M. J. Petrus, M. X. Zhu, A. Patapoutian, *Nat. Chem. Biol.*, 2009, **5(3)**, 183−190.

17. WHO, FAO, IAEA, *Trace elements in human health and nutrition*, Geneva, 2002.

18. Food and Nutrition Board, IOM, *Dietary reference intakes of vitamin A, vitamin K, arsenic, boron, chromium, copper, iodine, iron, manganese, molybdenum, nickel, silicon and zinc*, National Academy Press: Washington, DC, 2002.

20. W. Maret, *Metallomics*, 2015, **7(2**), 202−211.

21. E. M. Nolan, S. J. Lippard, *Acc. Chem. Res.*, 2009, **42(1)**, 193−203.

22. M. Formica, Vi. Fusi, L. Giorgi, M. Micheloni, *Coord. Chem. Rev.*, 2012, **256**, 170−192.

23. G. Piersanti, F. Remi, V. Fusi, M. Formica, L. Giorgi, G. Zappia. *Org. Lett.*, 2009, **11(2)**, 417−420.

24. M. Formica, V. Fusi, L. Giorgi, M. Micheloni, P. Palma, R. Pontellini, *Eur. J. Org. Chem.*, 2002, 402−404.

25. S. Amatori, G. Ambrosi, M. Fanelli, M. Formica, V. Fusi, L. Giorgi, E. Macedi, M. Micheloni, P. Paoli, R. Pontellini, P. Rossi, M. A. Varrese, *Chem.−Eur. J.*, 2012, **18**, 4274−4284.

26. V. Fusi, L. Giorgi, M. Formica, M. Micheloni, E. Macedi, G. Ambrosi, P. Paoli, P. Rossi, R. Pontellini, *Inorg. Chem.*, 2010, **49**, 9940−9948.

27. G. Ambrosi, C. Battelli, M. Formica, V. Fusi, L. Giorgi, E. Macedi, M. Micheloni, R. Pontellini, L. Prodi, *New J. Chem.*, 2009, **32**, 1−10.

28. S. Aoki, D. Kagata, M. Shiro, k. Takeda, E. Kimura, *J. Am. Chem. Soc.*, 2004, 126, 13377−13390.

29. J. L.Vinkenborg, T. J. Nicolson, E. A. Bellomo, M. S. Koay, G. A. Rutter, M. Merkx, *Nat. Methods*, 2009, **6**, 737−740.

30. T. Iijima, A. Momotake, Y. Shinohara, T. Sato, Y. Nishimura, T. Arai, *Phys. J. Chem. A*, 2010, **114**, 1603−1609.

31. J. E. Kwon, S. Lee, Y. You, K.-H. Baek, K. Ohkubo, J. Cho, S. Fukuzumi, I. Shin, S. Y. Park, W. Nam, *Inorg. Chem.* 2012, **51**, 8760−8774.

32. F. Marchetti, C. Pettinari, R. Pettinari, *Coordi. Chem. Rev.*, 2005, **249(24)**, 2909−2945.

33. P. A. Chavan, N. S. Dighe, S. R. Pattan, D. S. Musmade, M. S. Sanap, M. S. Kedar, P. P. Gadhave, *Pharmacologyonline*, 2010, **1(Newsletter)**, 180−189.

34. G. Varvounis, *Adv. Heterocycl. Chem.*, 2009, **9**8, 143−224.

35. C. Hui, L. Guangfei, L. Lang, J. Dianzeng, *Spectrochimica Acta, Part A*, 2005, **61**, 2590−2594.

36. D. J. Qian, W. N. Leng, Y. Zhang, Z. Chen, J. Van Houten, *Spectrochim. Acta, Part A*, 2000, **56**, 2645−2651.

37. A. R. Kurbangalieva, A. I. Movchan, O. N. Kataeva, I. A. Litvinov, G. A. Chmutova, *J. Mol. Struct*. 2001, **595**, 15−20.

38. C. Trujillo, G. Sanchez-Sanz, I. Alkorta, J. Elguero, *ChemPhysChem*, 2015, **16**, 2140−2150.

39. D. Caiming, A. Samat, L. Lang, W. Dongling, J. Dianzeng, Z. Rong, *Spectrochimica Acta, Part A*, 2015, **148**, 318−323.

40. S. Mantenuto, F. Mantellini, G. Favi, O. A. Attanasi, *Org. Lett.*, 2015, *17*, 2014−2017.

41. G. E. Dobretsov, T. I. Syrejschikova, N. V. Smolina, *Biophysics (English Translation)*, 2014, **59(2)**, 183−188.

42. L. Lang, X. Xiangyun, J. Dianzeng, G. Jixi, X. Xiaolin, *J. Org. Chem.*, 2010, **75**, 4742−4747.

43. B. Banu, S. Nurgül, S. Zeynel, *Tetrahedron Lett.*, 2015, **5**6, 2149–2154.

44. S. Katsuta, Y. Kudo, Y. Takeda, *Curr. Top. Solut. Chem.*, 1997, **2**, 219−251.

Table of Content

A series of hydroxypyrazole-based selective Zn(II) sensors were synthesized. One of them shows a double band-emission due to phototautomerism.